

Article

Multi-Layered Stratification in the Baltic Sea: Insight from a Modeling Study with Reference to Environmental Conditions

Bijan Dargahi ^{1,3,*}, Venkat Kolluru ^{2,*} and Vladimir Cvetkovic ³

¹ Division of Hydraulic Engineering, School of Civil and Architectural Engineering, KTH Royal Institute of Technology, 10044 Stockholm, Sweden

² Environmental Resources Management, Inc., 75 Valley Stream Parkway, Suite 200, Malvern, PA 19355, USA

³ Division of Water Resource Engineering, School of Civil and Built Environment, KTH Royal Institute of Technology, 10044 Stockholm, Sweden; vdc@kth.se

* Correspondence: bijan@kth.se (B.D.); venkat.kolluru@erm.com (V.K.); Tel.: +46-484-913-0393 (B.D.)

Academic Editor: Richard P. Signell

Received: 18 July 2016; Accepted: 7 December 2016; Published: 7 January 2017

Abstract: The hydrodynamic and transport characteristics of the Baltic Sea in the period 2000–2009 were studied using a fully calibrated and validated 3D hydrodynamic model with a horizontal resolution of 4.8 km. This study provided new insight into the type and dynamics of vertical structure in the Baltic Sea, not considered in previous studies. Thermal and salinity stratification are both addressed, with a focus on the structural properties of the layers. The detection of cooler regions (dicothermal) within the layer structure is an important finding. The detailed investigation of thermal stratification for a 10-year period (i.e., 2000–2009) revealed some new features. A multilayered structure that contains several thermocline and dicothermal layers was identified from this study. Statistical analysis of the simulation results made it possible to derive the mean thermal stratification properties, expressed as mean temperatures and the normalized layer thicknesses. The three-layered model proposed by previous investigators appears to be valid only during the winter periods; for other periods, a multi-layered structure with more than five layers has been identified during this investigation. This study provides detailed insight into thermal and salinity stratification in the Baltic Sea during a recent decade that can be used as a basis for diverse environmental assessments. It extends previous studies on stratification in the Baltic Sea regarding both the extent and the nature of stratification.

Keywords: Baltic Sea; hydrodynamics; modeling; vertical structure; stratification; dicothermal; GEMSS

1. Introduction

The Baltic Sea is a brackish sea located in northern Europe from 53° N to 66° N latitude and from 20° E to 26° E longitude. It is connected to the Atlantic Ocean via the Danish Straits. The Baltic Ice Lake was born 13,000 years ago and its present brackish state emerged 7000 years ago. For 2000 years, the salinity has been close to the present level (mean salinity: 7 parts per thousand). The Baltic Sea borders nine coastal countries with a total population of 85 million people (see Figure 1, [1]). The maximum length and width are 1600 km and 193 km, respectively. The surface area is 377,000 km², with an average depth of 55 m and a water volume of 20,000 km³. Its maximum depth is 459 m, which is located between Stockholm and the Island of Gotland. The Baltic Sea is a shallow sea that consists of a series of basins interconnected through narrow sills (Figure 2).

In spite of the Baltic Sea HELCOM agreement signed in 1974, the state of the Baltic Sea has worsened (<http://www.helcom.fi>). Nutrient levels in the water and sediments are high, and poor oxygen conditions and “dead bottoms” exist in large archipelago areas of both Sweden and Finland [2].

However, during the past few decades there have been considerable efforts towards better and more sustainable management of the Baltic Sea. Here, the hydrodynamics of the Baltic Sea, which has been the subject of intensive research since the 1930s, plays a major role. The number of available journal articles and other publications exceeds several hundred. The foci of these studies are exchange processes, especially salt transport from the North Sea, and water age. Some of the main contributors are Meier [3], and Lehman and Hinrichsen [4]. Here, the work of Omstedt et al. [5] should be mentioned as it presents the state of knowledge on various hydrodynamic features of the Baltic Sea. There are also several excellent books covering many different aspects, including Feistel et al. [6], Leppäranta and Myrberg [7], and Harff et al. [8]. For a general literature review, the interested reader is referred to the comprehensive review given by Dargahi and Cvetkovic [9].



Figure 1. The Baltic model region and the model open boundary location [1].

The present study concerns the hydrodynamics of the Baltic, with a focus on the details of stratification, which is the primary feature of the sea. The novel features of the work are the relatively long simulation period of 10 years and the use of a complete set of external boundary conditions with maximum spatial and temporal resolution, in combination with highly accurate bathymetry. The main objectives were to create an accurate and validated 3D hydrodynamic model for investigating specific stratification characteristics that have not been addressed in the previous studies. In the following paragraph we present a short summary of previous research works on stratification.

The Baltic Sea is highly stratified by strong vertical salinity and temperature gradients. The stratification is commonly referred to as a two-layer structure that consists of an upper and a lower layer. A transitional middle layer exists between the upper and lower layers, which are known as halocline and thermocline, respectively. There is a significant variation in the depth of the halocline, from 40 m to 80 m in deeper regions to 10 m–30 m in shallower regions [7]. The lower values are found in the Gulf of Riga (mean value = 25 m), and Arkona Basin, with a mean value of 25 m for both regions [10,11]. The surface salinity varies in the north with a mean value of 3 ppt (parts per thousand) to 8 ppt to the south, i.e., the Arkona Basin. The corresponding mean value at the lower layer is in the range of 4–12.5 ppt. However, the salinities are considerably higher in the open sea. The mean values

in the Kattegatt (the region in which the Baltic Sea drains through the Danish strait) are 22 ppt and 31 ppt, respectively (same references). Suominen et al. [12] studied surface salinity gradients and their temporal fluctuations in the Archipelago Sea of the northern Baltic Sea based on field salinity data for the time period July 2007–August 2008. They identified a broad scale gradient from low salinity in the shallow inner bays to the high salinity in the open sea areas towards the Baltic proper. The steepest gradients were observed in the semi-closed part of the archipelago. One important result was that the use of temporal mean values of salinity was insufficient for coastal management purposes in the region.

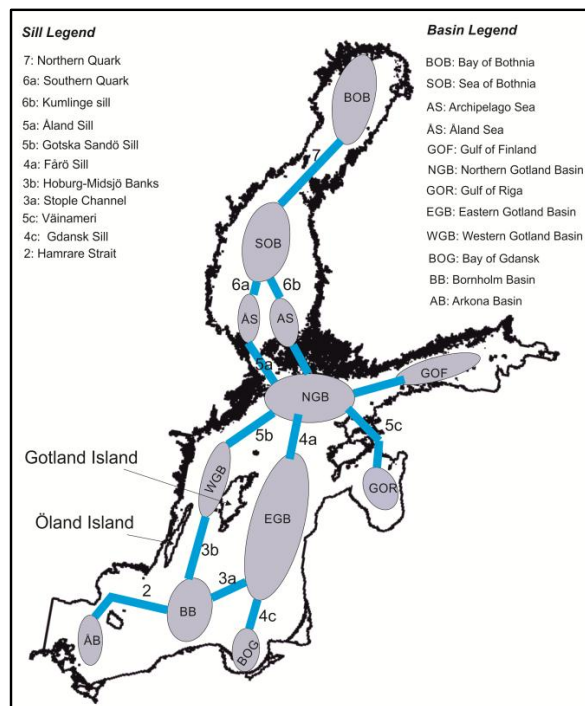


Figure 2. The Baltic Sea basin system, redrawn from an interpolated figure by Leppäranta & Myrberg [7].

The halocline depth is controlled by wind-induced mixing and advection, which appears to change little over time. Väli et al. [11] looked into variations of the halocline during 1961–2007. Two periods were identified with shallow halocline during 1970–1975, and with deep halocline during 1990–1995. The main conclusion was that the freshwater content and absolute wind speed control the halocline depth in the Baltic Sea. However, they found the wind speed to have a moderate impact on the mean halocline depth in the Baltic proper due to the low impact of runoff.

An important issue is the effect of fresh water on stratification in the Baltic Sea. Hordoir and Meier [13] studied the dynamics of fresh water, which is released during spring into the Baltic proper. They showed that the fresh water only reaches the center of the Baltic proper after late summer. A small amount of fresh water may reach the entrance of the Baltic Sea during one season. The arrival of fresh water increases vertical stratification, which can in turn trigger the onset of the spring blooms. They also found that the seasonal changes in the fresh water outflow were closely connected with those of the zonal wind. An important result was the correlation of the annual variability of the seasonal freshwater outflow maximum with the North Atlantic Oscillation.

The temperature stratification in the Baltic Sea has a mean three-layer structure in analogy to the salinity stratification. The layers are commonly referred to as the epilimnion (upper layer), thermocline (middle layer), and hypolimnion (lower layer). In similarity with the other large water bodies, there is a seasonal stratification cycle, which is driven by the variations in the energy balance. However, in the case of the Baltic Sea there are two specific features. First, fall and spring overturns are not well

defined, and second, the hypolimnion has a nearly constant temperature, with few seasonal variations. During the winter periods, the epilimnion layer has a lower temperature than the hypolimnion layer. The Baltic Sea is monitored using 22 stations, as shown in Figure 3. A typical temperature difference at the gauge station BY15 is about 5 °C. In the spring, following the ice melt, a thin warmer surface layer rapidly develops and sets up the thermocline. The thickness of the layer varies considerably from north to south, but a mean value of about 15 m can be used. The temperature gradient is high within the epilimnion layer. For instance, at BY15, the temperature can vary from 1.5 °C to 5 °C within a depth of 60 m. Below this depth, the temperatures increase rapidly to reach the constant temperature of the hypolimnion layer (about 5 °C). The layer with transitional temperature is known as the dicothermal layer, which is a cold layer sandwiched between two layers with higher temperatures (dicothermal). The dicothermal layer was first discovered by the Ekman expedition of 1877 to the Baltic Sea (see Fonselius [14]). The layer appears to originate from the vertical convection of the surface water in the winter. It is further explained that this cold surface water from the previous winter was preserved between the thermocline and halocline (see Fonselius [14]). The dicothermal layer develops at high latitudes with cold climates. Peter [15] reports the development of a layer with a thickness of 100 m in the Indian Ocean region of the Antarctic. The reported thickness in the Baltic Sea is in the range of 5–30 m, which persists during the summer and disappears during the autumn [7]. Here, we note that the measured temperature profiles in the southern basins confirm the formation of the dicothermal layer even during the spring.

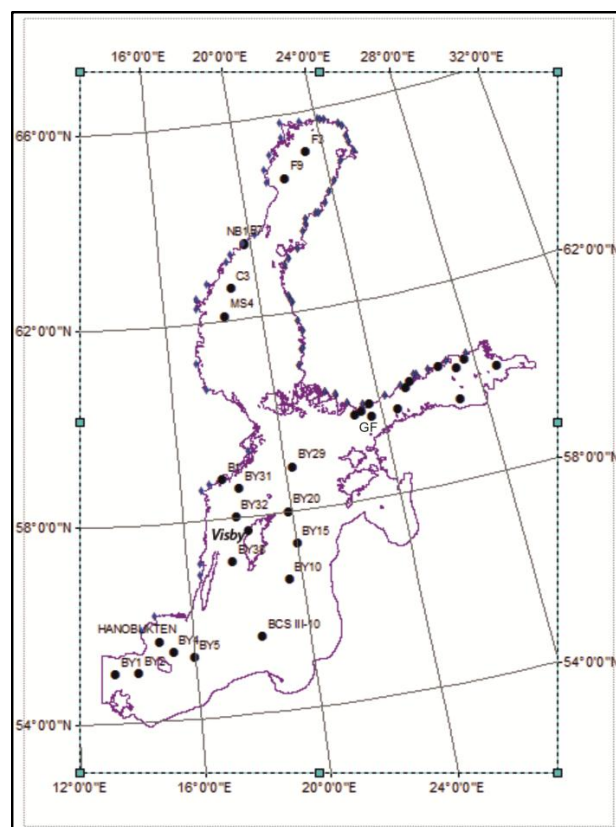


Figure 3. Map showing the monitoring stations in the Baltic Sea.

The stratification is strongest during the summer due to high solar radiation input and warm air temperatures. The surface layer thickness increases to about 20 m during the summer period due to wind induced vertical mixing. The temperature within the layer is nearly constant. Below the surface layer, a strong thermocline develops that has a sharp temperature drop of about 10 °C over a depth of about 10 m (e.g., temperature profile at BY15). There is also a dicothermal layer below the

thermocline, which has a thickness of about 30 m at BY15. The hypolimnion layer has a relatively constant temperature of 4–5 °C, which is close to the temperature of maximum density of water. The layer thickness varies considerably, from about 30 m in shallow regions to 100 m in the deeper region. The negative effect of the strong stratification limits the exchange between the epilimnion and hypolimnion layers.

During autumn, the surface heat losses start to increase and the thermocline depth deepens. For instance, in the Eastern Gotland Basin, the thermocline reaches a depth of about 40 m. The lower temperatures cause the temperature gradient to decrease, which in turn weakens the thermocline. The temperature changes in the thermocline cause a weak positive temperature gradient to develop in the hypolimnion layer (e.g., 1 °C over 100 m).

2. Materials and Methods

The materials used to model the Baltic Sea consisted of basic geometrical and various flow and meteorological data for the period 2000–2009 as listed below.

- The shoreline and the bathymetry in GIS format.
- Daily flow discharges for 24 Swedish rivers, 38 Finnish rivers, and five Eastern European rivers (i.e., the Daugava, Neman, Neva, Odra, and Vistula).
- Monthly mean flow discharge for four Eastern European rivers (i.e., Lielupe, Narva, Pärnu, and Narva). The daily records were not available.
- Water temperature for all the rivers.
- The forcing meteorological data (air temperature, dew point, cloud cover, pressure, wind speed, and wind direction) at 3-h intervals as grid data.
- Precipitation as rain intensity at 19 stations at daily intervals.
- Water quality data at 15-day intervals for 22 different stations spread across the sea. The data included water temperature, salinity, dissolved oxygen, and phosphorous.
- Wave heights and sea and water levels at several stations across the sea.

The main data sources were the Swedish Meteorological and Hydrological Institute, SMHI [16], and the Finnish Meteorological Institute, FMI [17]. The gridded meteorological data were obtained from <http://www.smhi.se/en/research/research-departments/analysis-and-prediction>, computed based on actual measurements. Among the many variables that affect the hydrodynamics of a large water body, the bathymetry and inflow of freshwater are the most important. So, special attention was paid to improving the quality and reliability of the bathymetry data.

The digitized bathymetry data for the Baltic Sea were obtained from the Leibniz Institute for Baltic Sea Research [18]. This dataset was frequently used in previous models of the Baltic Sea and also agrees well with published bathymetry maps. This dataset performed poorly in resolving the various channels along the coastlines of Finland, and in the Stockholm archipelago. The Åland Sea and its archipelago were also poorly reproduced. The latter problems caused a significant flow blockage in the forenamed areas. To resolve the foregoing issues, the bathymetry had to be refined using several different resolutions ranging from 50 m to 400 m that depended upon the model regions. The focus was on the areas along the coastlines and the interconnected channel systems. The modifications were done by a combined method using published maps and other databases in ARCGIS. The final bathymetry was analyzed using standard statistical methods to gain an understanding of the depth distribution and its relationship for resolving the vertical layers for the study domain. It was observed that depths less than 100 m cover 80% of the sea. This is an important result since it indicates the need for finer vertical grid resolution within the depth of 0–100 m.

2.1. Model Description

A three-dimensional, time-dependent hydrodynamic model, GEMSS[®] (Generalized Environmental Modelling System for Surface waters), was used. GEMSS was developed and maintained by Environmental Resources Management, Inc., Malvern, PA, USA. GEMSS is an integrated system of 3D hydrodynamic and transport models embedded in GIS. GEMSS is in the public domain [19] and has been used for similar studies throughout the United States and worldwide. Edinger and Buchak [20,21] first presented the theoretical basis of the model. The model was enhanced by implementing higher-order transport schemes, construction of various constituent modules, incorporation of various supporting software tools, GIS interoperability, visualization tools, graphical user interface (GUI), and post processors [22–26].

The hydrodynamic and transport relations are developed from the horizontal momentum balance, continuity, constituent transport and the equation of state. A detailed mathematical formulation of the model both in the hydrostatic and non-hydrostatic forms is described in [17,19] so will not be repeated here. The hydrodynamic equations are semi-implicit in time, have the advantage of computational stability, and are not limited by the Courant condition. The vertical momentum dispersion coefficient and vertical shear are evaluated from a Von Karman relationship modified by the Richardson number. Higher-order turbulence closure schemes (two-equation model, and second-moment closure model by Mellor and Yamada [27] are also included. The Two-Equation model used in GEMSS is based on the Generic Length Scale (GLS) model proposed by Umlauf and Burchard [28], and by Warner et al. [29]. The longitudinal and lateral coefficients are scaled to the dimensions of the grid cell using the dispersion relationships field developed by Okubo [30] and modified to include the velocity gradients using the Smagorinsky [31] relationship. The wind stress and bottom shear stress are computed using quadratic relationships with appropriate friction coefficients.

The transport module can run in fully explicit to fully implicit modes in a vertical direction while performing explicit computations in a horizontal direction [32]. GEMSS uses a curvilinear variably spacing horizontal staggered finite difference grid, which is based on control volume, with the elevation and constituent concentration computed at cell centers and velocities through a cell interface. Z-level with variable thickness is used for defining the grid in the vertical direction. Additional details of the model can be found in the technical documentation of GEMSS [32–35].

The wave dynamic module of GEMSS has two wave models, i.e., a steady state linear and a non-linear model. In the present investigation, the non-linear model was used. The model accounts for the wave influence on the bottom shear stresses by using the Madsen and Grant [36] equation. In the current study, a simplified linear ice model that relates the growth of ice thickness to the temperature differences between water and melting ice, and ice in equilibrium was used. Based on sensitivity studies, the linear ice model is a reasonably good model for the present study, which was run for a long period of time to understand the hydrodynamic characteristics. In addition, the particle tracking module of GEMSS was used for the current study to understand the travel time, water age [37] and vertical mixing processes at various basins in the Baltic Sea using the current persistency index defined in [38].

The GEMSS model was recently used by the first author to investigate the hydrodynamic and related water quality characteristics of Saltsjo [33] and Lake Tana in Ehiopia [34].

2.2. Model Setup

The model setup involved several main steps of creating the model grid, interpolating the bathymetry into the grid, defining the boundary conditions that include river inflow, water levels, precipitation, and forcing meteorological conditions.

The model grid was created using the grid generator tool of GEMSS[®]. A non-uniform boundary-fitted curvilinear grid in a horizontal plane (x - y) with a non-uniform z -layering in the vertical plane was created for the study domain and is shown in Figure 4. The grid dimensions are 195×200 , with an approximate cell size of 4.8 km. The final bathymetry described in the previous section was used to interpolate the depths for each grid cell in the study domain. Since depths less than

100 m cover almost 80% of the Baltic Sea, the vertical layers were designed to have a finer resolution within this depth. The total number of vertical layers used in the current study was 47, with thicknesses varying from 1.5 m to 12 m.

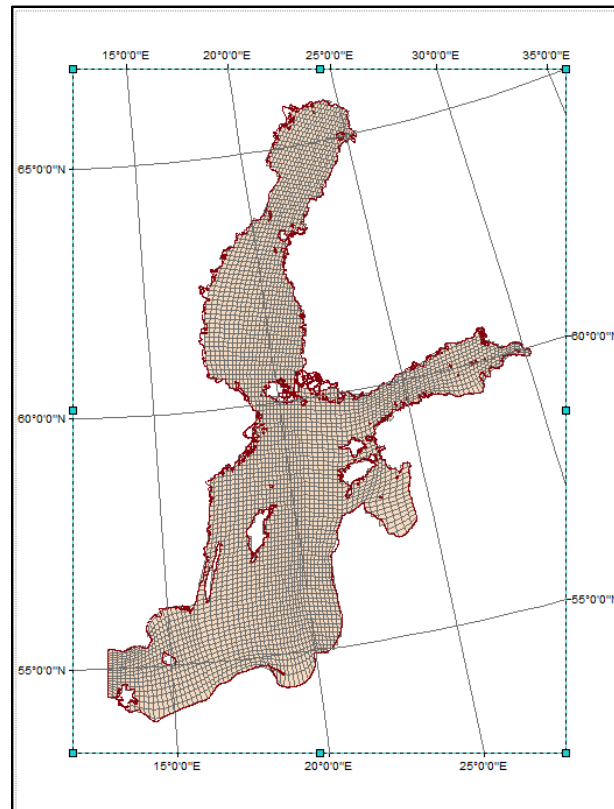


Figure 4. The Baltic Sea numerical model grid.

2.2.1. Input Data

The model boundary conditions consisted of discharge, head (water levels), precipitation, and meteorological forcing conditions. The true dynamic character of the input data is an important issue that directly affects the results of any hydrodynamic simulations. Here, the input data are the river discharge hydrographs and the forcing meteorological conditions. The amplitude and frequency of the data control various hydrodynamic properties such as stratification and mixing processes. The control file generator tool of GEMSS was used to define all forcing data needed for the current study.

The discharge boundary conditions were defined for 69 rivers out of 72 that enter the modeled region. To define the exact locations of the rivers, a GIS file was used. The river data included the flow discharge, water temperature, and salinity. We assumed that the rivers enter through the water surface grid in the model.

The water level was set at the open boundary with the North Sea, as shown in Figure 1 with a red line (≈ 104 km wide). The GPS coordinates are $54^{\circ}28' N 12^{\circ}50' E$ and $55^{\circ}22' N 13^{\circ}03' E$ in the south and north directions, respectively. To set the water level, the data at the gauge station Skanör ($55^{\circ}26' N 12^{\circ}50' E$) were used. At the open boundary the water temperatures and salinity profiles from monitoring station BY1 (see Figure 3) were used.

The precipitation data in mm/day were applied regionally by dividing the Baltic Sea surface into 19 regions, each with its corresponding rain intensity. Both point and gridded data were used for meteorological forcing conditions. The gridded data cover the whole Baltic drainage basin with a grid of ($1^{\circ} \times 1^{\circ}$) squares. The grid extends over the area: Latitude 49.5° – 71.5° N, Longitude 7.5° – 39.5° E. The gridded data covers 32 years, starting in 1970. The gridded meteorological data

represent geostrophic wind and were converted to the open surface wind speed needed for the model using the 2/3 power law. The second set was point data, which are available mainly along the coastlines.

2.2.2. Initialization

The model initialization is an important part of any hydrodynamic simulation, especially in the case of large water bodies such as the Baltic Sea. The long residence times make the model output sensitive to the choice of method. In the present study, we initiated the model using the data available at all the monitoring stations for water temperature and salinity. A total of 22 monitoring stations (see Figure 3) were used to interpolate temperature and salinity for the entire model grid at the start of the model simulation on 1 January 2000.

2.3. Simulations

In the present study we used the following setups for both partial and complete simulations, i.e., one year and 10 years.

- Vertical dispersion: Two-Equations with Mellor–Yamada formulation.
- Mixing dispersion: Okubo formulation.
- Transport diffusion: Prandtl method.
- Surface heat exchange: term by term, defining all the heat source and sink terms with atmospheric interaction.
- Transport model: Quick.
- Vertical momentum: Non-hydrostatic.
- Coriolis force: Using model grid.

The maximum time step used in the model simulations was 360 s. The auto time step feature available in GEMSS[®] was used so that the model time step goes only below the maximum time step due to extreme forcing conditions such as large wind speeds and river discharges. The calibration and verification simulations were carried out on a 4.8-km model grid shown in Figure 4. The model was run for the year 2000 for calibration. The model validation was done for the full 10 years using the restart files created by the calibration run.

3. Results

3.1. Model Calibration & Validation

A detailed description of model calibration and verification is available in [9] and will not be repeated here. Instead, it will be briefly described here using some relevant plots and tables.

The model calibration for year 2000 was done using all the 22 monitoring stations shown in Figure 3. The temperature, salinity, and water levels field data were used. It involved a systematic two-step approach with a focus on temperature and salinity profiles. The first step was initiating the model using the data available at all the monitoring stations for water temperature and salinity. The RMS (Root Mean Square) errors of temperature and salinity were then evaluated. In Step 2 the model was re-run with new sets of initial data that were successively adjusted to lower the RMS values. The procedure significantly improved the agreement with the measurements, with a relative error range of 10%–20% for both temperature and salinity. During the calibration procedure, the bottom friction coefficient, wind drag coefficient, and coefficients related to surface heat exchange processes were adjusted to lower the RMS values with respect to field observations. The coefficient values used for the calibration matched reasonably well with similar modeling exercises completed for the Baltic Sea. Based on all the calibration adjustments we have done for various model parameters, we found that establishing the appropriate horizontally and vertically varying initial condition was the most important precursor to achieve low RMS values on model results. The model successfully captured

the seasonal variations in water temperature and salinity profiles as well as the stratification across the entire Baltic Sea. Here, we have chosen only some typical results for a few stations. Figures 5 and 6 show the combined temperature and salinity profiles at the monitoring stations F3, GF, BY15, and BY5. Table 1 summarizes the absolute and mean relative errors at these monitoring stations. The range of the error is 4%–10%, which is acceptable considering the large volume of the Baltic Sea and its complex hydrodynamics.

Table 1. Calibration error summary for temperature and salinity.

Time	Absolute Error								Mean Relative Error %	
	14 January 2000		28 May 2000		18 August 2000		9 November 2000		T	S
Station	T (°C)	S (ppt)	T (°C)	S (ppt)	T (°C)	S (ppt)	T (°C)	S (ppt)		
F3	0.15–0.6	0.1–0.2	0.1–1.5	0.1–0.2	0.1–0.2	0.1–0.2	0.1–0.2	0.1–0.2	10	3
Time	14 January 2000		28 May 2000		22 August 2000		25 October 2000			
BY15	0.1–0.57	0.1–0.8	0.1–1.3	0.1–0.8	0.1–0.9	0.1–0.7	0.1–1.6	0.1–1.2	4	4
Time	14 January 2000		28 May 2000		22 August 2000		25 October 2000			
BY5	0.1–0.2	0.1–0.2	0.1–0.5	0.1–0.3	0.1–0.5	0.1–0.3	0.1–1.6	0.1–2	5	6
Time	2 January 2000		6 June 2000							
GF	0.1–1	0.1–0.7	0.1–1	0.1–0.2					9	8

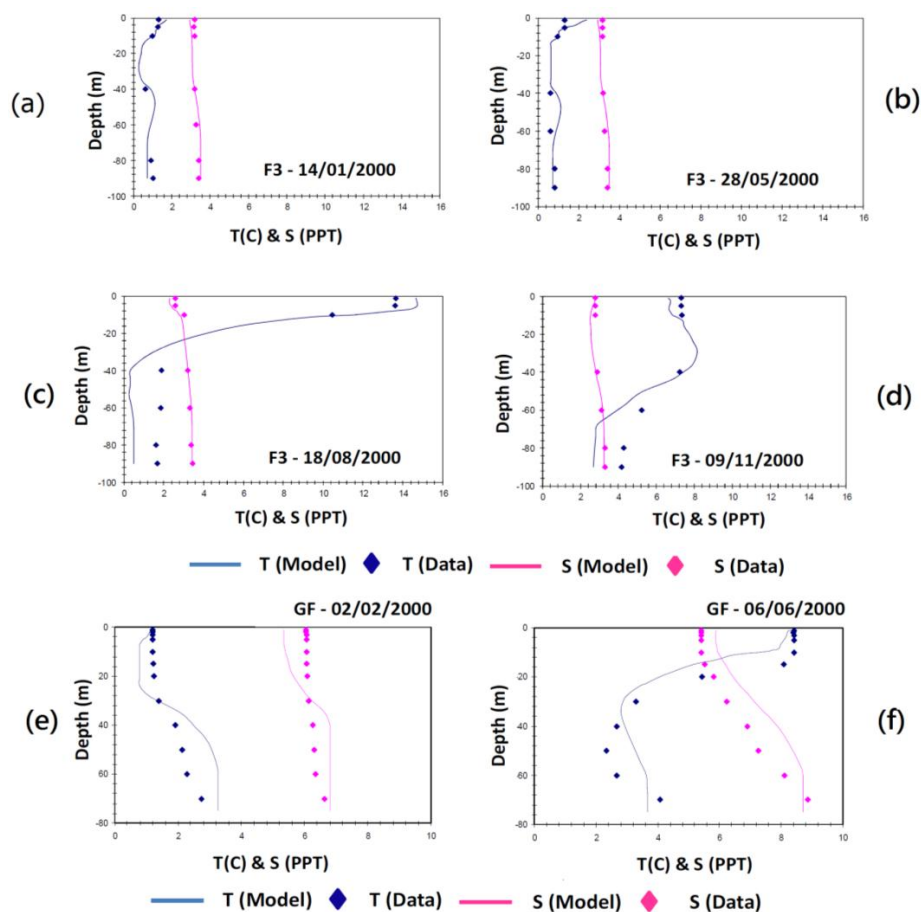


Figure 5. Comparison of model predicted vertical temperature and salinity profiles at the monitoring stations F3 (Bay of Bothnia) and GF (Gulf of Finland) with field measurements for the year 2000. (a) Station F3—14/01/2000; (b) Station F3—28/05/2000; (c) Station F3—18/08/2000; (d) Station F3—09/11/2000; (e) Station GF—02/02/2000; Station (f)—06/06/2000.

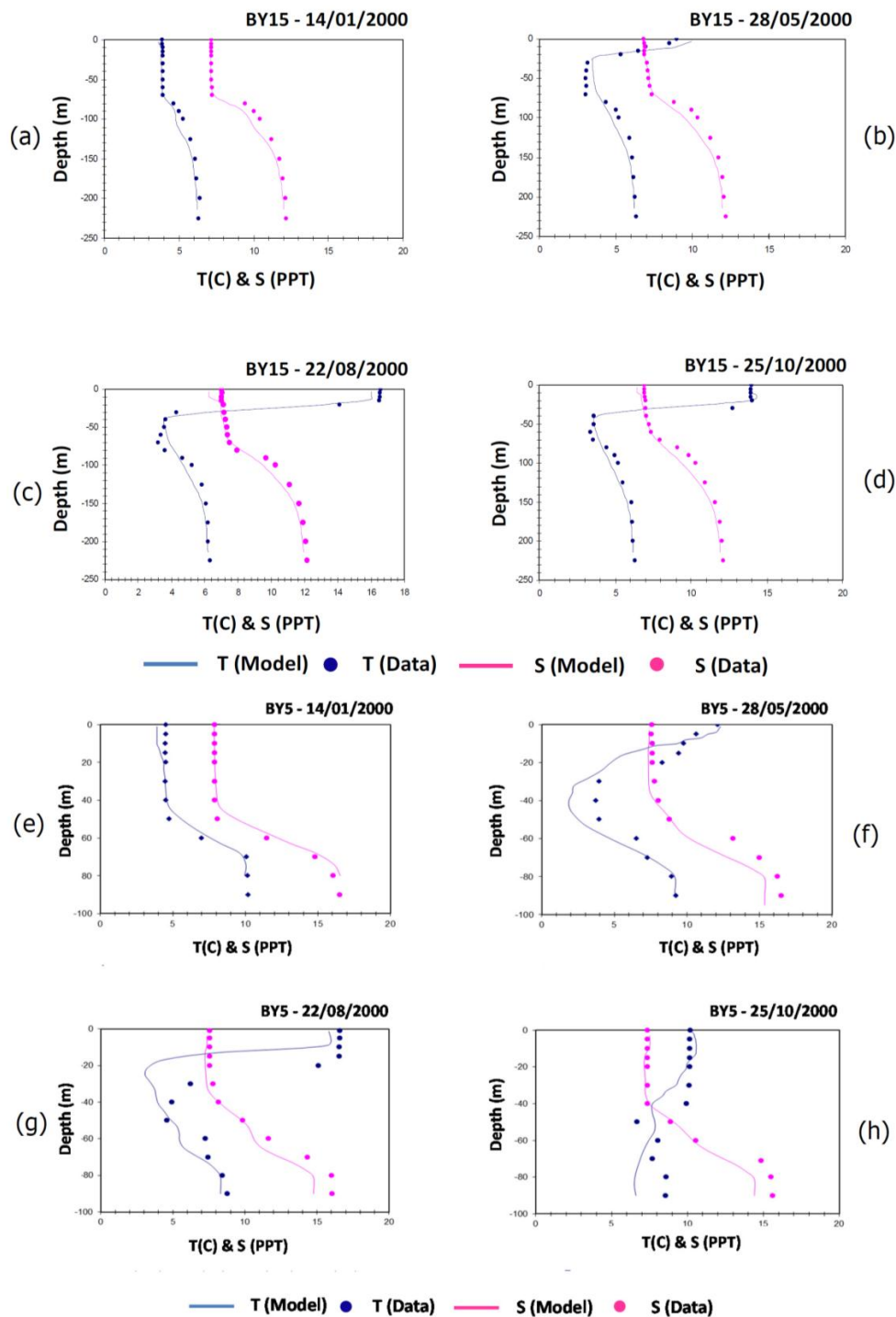


Figure 6. Comparison of model predicted vertical temperature and salinity profiles at the monitoring stations BY15 (Eastern Gotland Basin) and BY5 (Arkona Basin) with field measurements for the year 2000. (a) Station BY15—14/01/2000; (b) Station BY15—28/05/2000; (c) Station BY15—22/08/2000; (d) Station BY15—25/10/2000; (e) Station BY5—14/01/2000; (f) Station BY5—28/05/2000; (g) Station BY5—22/08/2000; (h) Station BY5—25/10/2000.

Model validation was done for the whole 10 years using the restart files created by the calibration simulation for the year 2000. For this purpose, the complete sets of field data at all the monitoring stations were used (Figure 3). These data were considered independently from the simulation results as only the first day records were used in the calibration simulations.

The model predictions of water temperatures and salinities were satisfactory at all the monitoring stations. Here, we have chosen some representative results for only a few stations. The time history plots in Figures 7 and 8 compare the model predicted temperature and salinity with the field data at stations F3 and BY29 at water surface and 40 m depth.

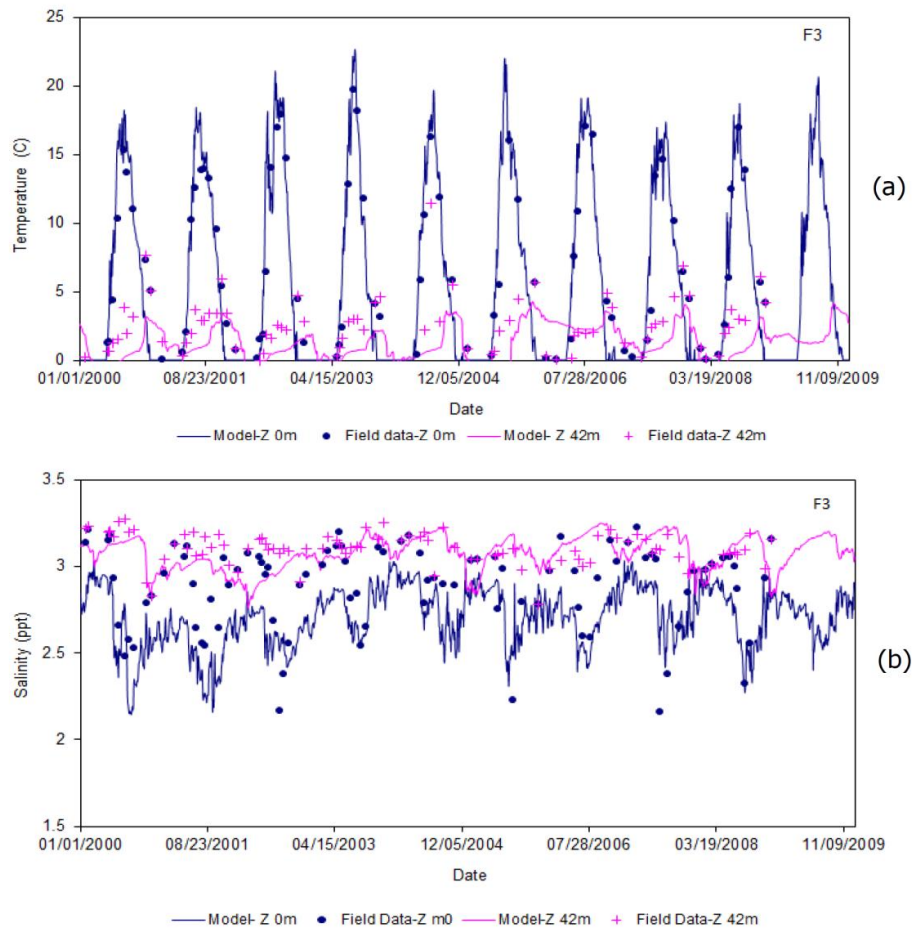


Figure 7. (a) Comparison of model predicted and measurements of temperature in the Baltic Sea at the Station F3 surface and 42 m depth for the time period 2000–2009; (b) Comparison of model predicted and measurements of salinity in the Baltic Sea at the Station F3 surface and 42 m depth for the time period 2000–2009.

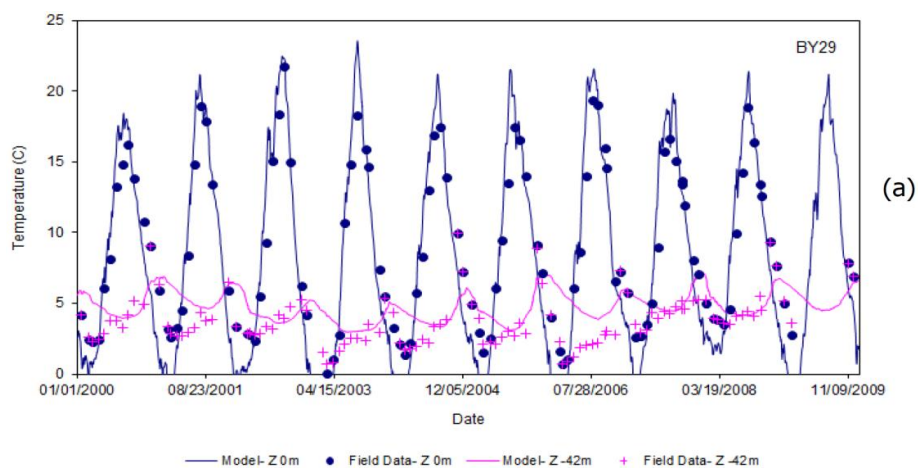


Figure 8. Cont.

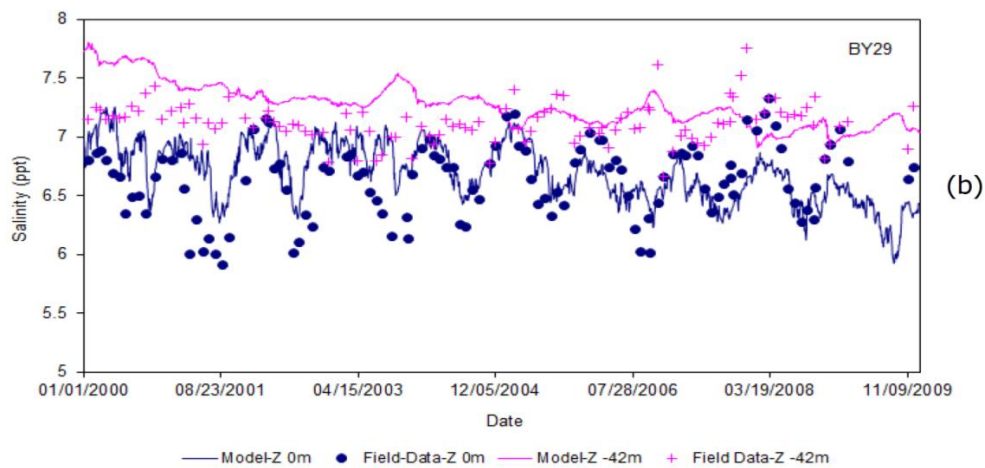


Figure 8. (a) Comparison of model predicted and measurements of temperature in the Baltic Sea at the Station BY29 surface and 42 m depth for the time period 2000–2009; (b) Comparison of model predicted and measurements of salinity in the Baltic Sea at the Station BY29 surface and 42 m depth for the time period 2000–2009.

The time history plots in Figure 9 compare the model predicted salinity with the field data at stations BY15 and BY5. The comparisons are shown at the water surface and at the deepest points in the basins. The agreements for these stations are better than the other stations as they are closer to station BY1, which defines the model boundary condition.

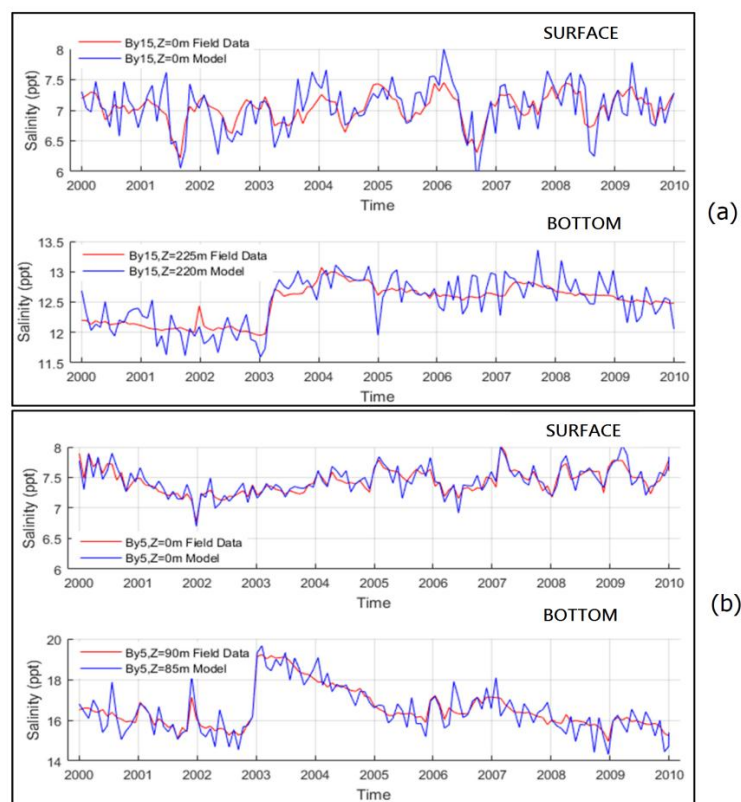


Figure 9. (a) Comparison of model predicted and measurements of salinity in the Baltic Sea at the Station BY15 surface and bottom for the time period 2000–2009; (b) Comparison of model predicted and measurements of salinity in the Baltic Sea at the Station BY5 surface and bottom for the time period 2000–2009.

The range of Nash–Sutcliffe coefficients [39] calculated for all the monitoring stations was 0.72–0.83, respectively, also suggesting close agreement. One other important feature is the ability of the model to capture the 10-year seasonal variations of water temperatures and salinities. The conclusion is that the model is reasonably validated over a considerable period, with a maximum relative error of 10%.

3.2. Stratified Vertical Structure

We used the validated model to investigate the stratified structure within all the basins of the Baltic Sea for the time period 2000–2009. The complete sets of numerical results are too extensive to be reported here. We will present and discuss some general results that are illustrated using a few plots (i.e., temperature and salinity) in both horizontal and vertical sections. The latter were investigated along several cross sections shown in Figure 10 that were selected to cut through all the basins (see Figure 2 for basin names) included in this study. The structure concerns thermocline and halocline stratifications, which are controlled by the hydrodynamic variables, forcing meteorological parameters, the topography, the shorelines, and the exchange processes with the North Sea.

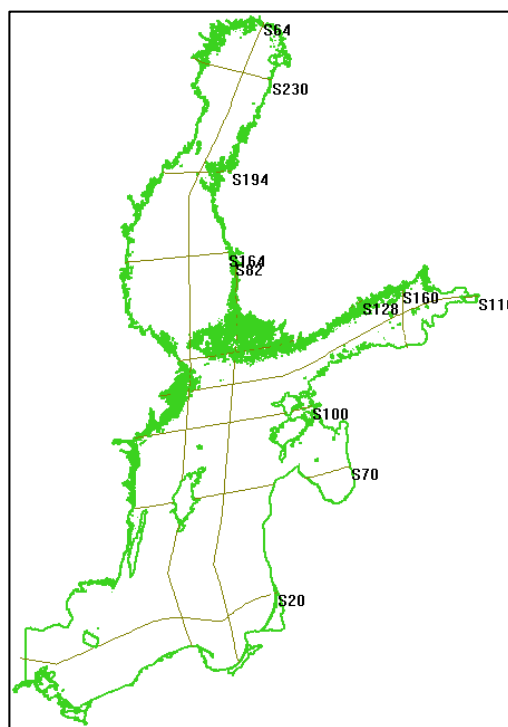


Figure 10. Selected cross sections in the Baltic Sea for vertical structure analysis.

Examples of simulation results for temperature and salinity are presented seasonally for winter (15 January), spring (15 May), summer (15 August), and autumn (15 October). Figures 11 and 12 show the surface and bottom contour plots of temperature for the year 2000, respectively. The typical cross-sectional plots of temperature are given for sections S64 and S116 for the year 2000 are given in Figures 13 and 14. The basins' abbreviated names are also given in the foregoing figures. It should be noted that the plotting scales were adjusted to show the full range of the hydrodynamic variables. This is particularly important for insuring that the stratification features are not obscured by the choice of the color scales. The summary results for all nine basins are presented in Tables 2 and 3. In these tables the layer thicknesses are normalized (L_n) with mean depth.

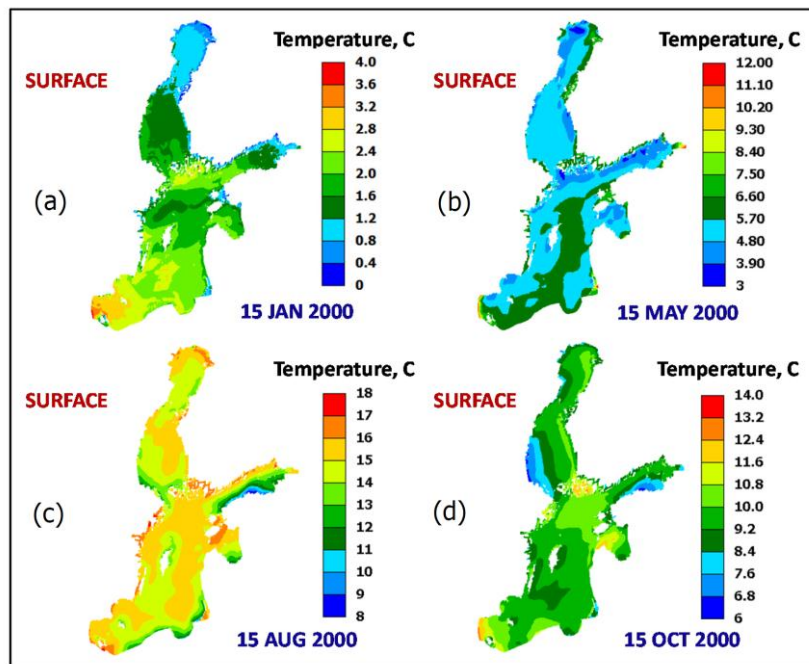


Figure 11. Seasonal surface temperature contour plots for the year 2000. (a) Winter; (b) Spring; (c) Summer; (d) Autumn.

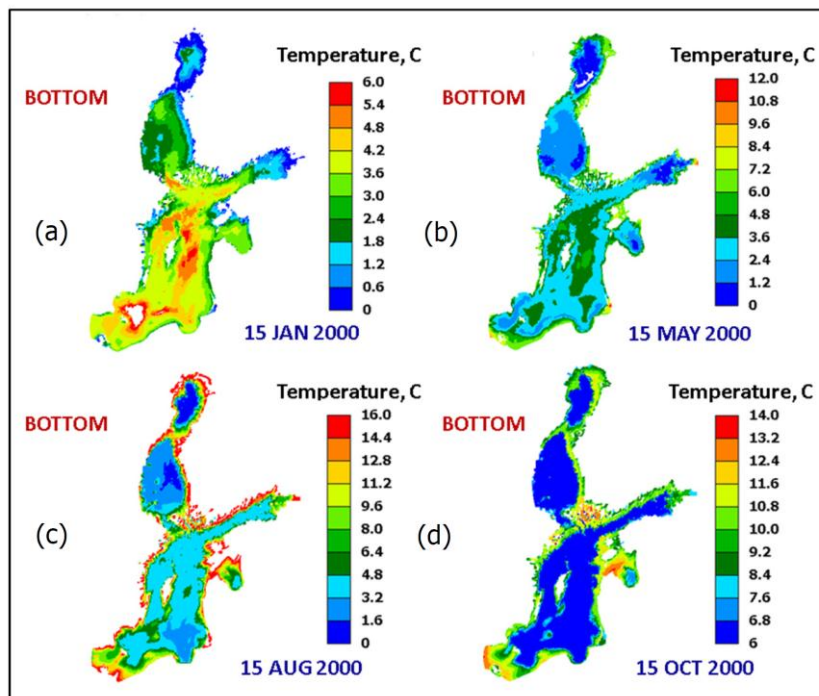


Figure 12. Seasonal bottom temperature contour plots for the year 2000. (a) Winter; (b) Spring; (c) Summer; (d) Autumn.

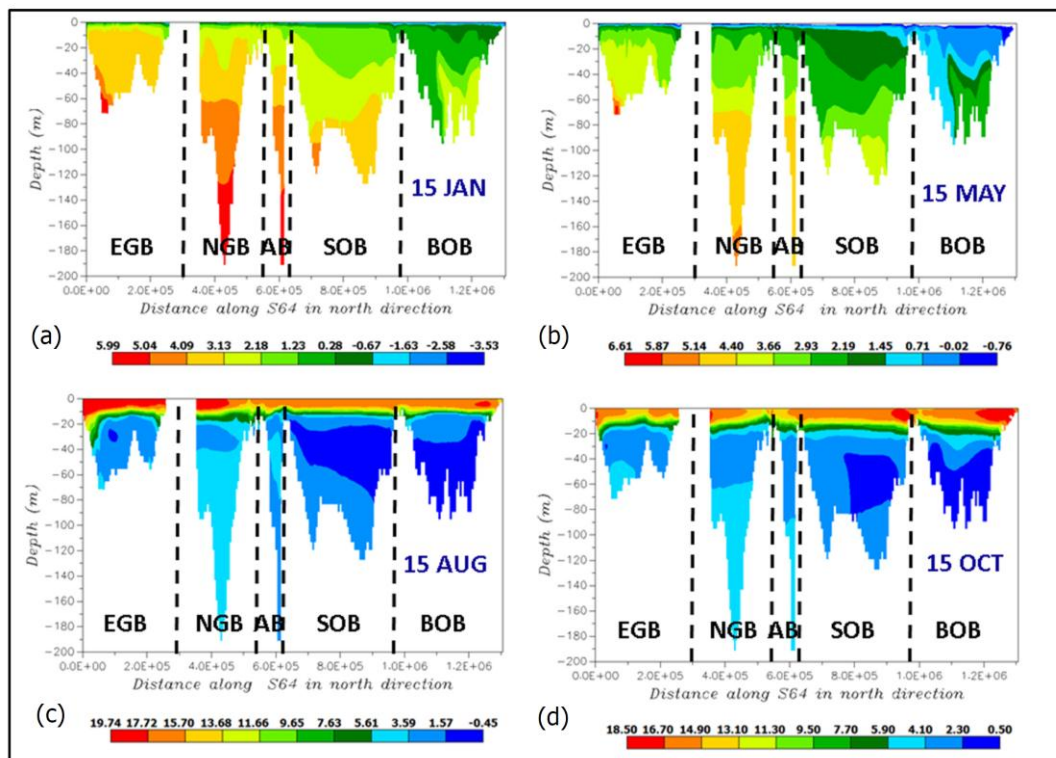


Figure 13. Seasonal thermal stratification plots in the Baltic Sea at cross section S64 for the year 2000. (a) Winter; (b) Spring; (c) Summer; (d) Autumn.

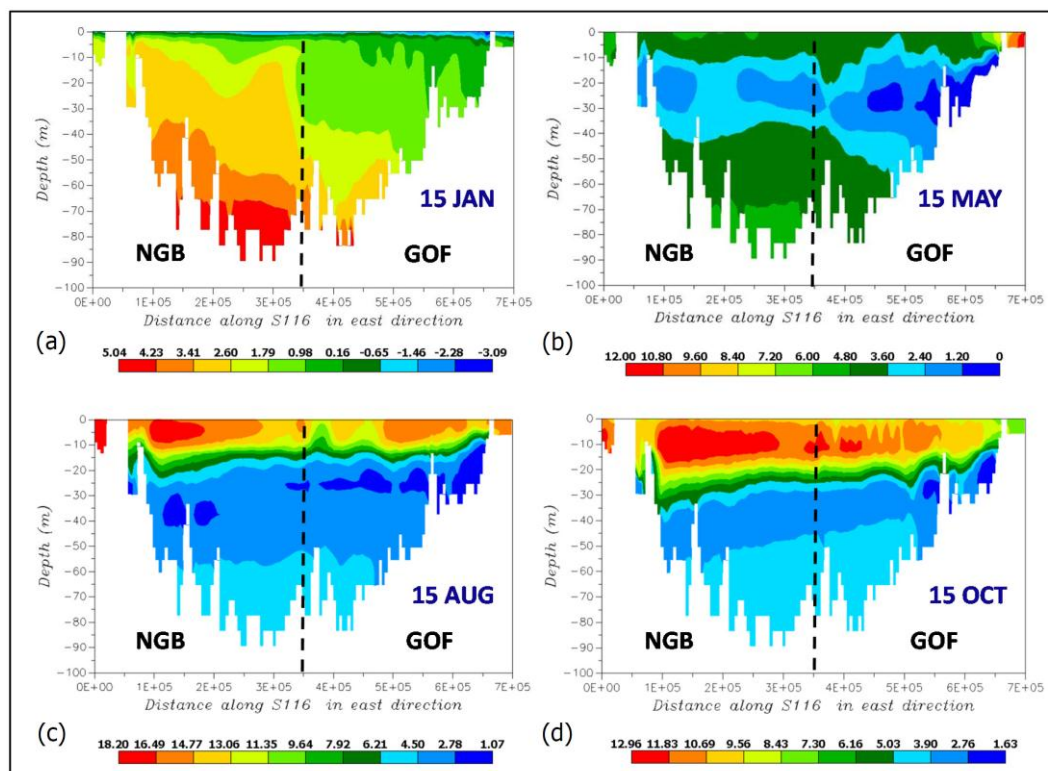


Figure 14. Seasonal thermal stratification plots in the Baltic Sea at cross section S116 for the year 2000. (a) Winter; (b) Spring; (c) Summer; (d) Autumn.

The temperature development at the Baltic Sea is affected by the intrusion of the warmer water masses from the North Sea and cold low salinity river water masses that flow into the Bay of Bothnia. The northern part of the Baltic Sea is covered by ice during winter and spring, which reduces the water temperature well into the summer. Figure 11 shows the seasonal variations of water temperature at the surface and bottom layers. The surface temperatures are in good agreement with the SMHI measurements available in [40]. The surface temperatures vary in the range of 0 °C to 18 °C. In the winter, the bottom temperatures are higher than the surface temperatures by several degrees. The spring is marked by higher surface temperatures, with the exception of the Bay of Bothnia and the eastern Gulf of Finland. The surface temperatures increase significantly during the summer and are about 2 °C higher than the bottom layer temperatures. The autumn shows a transitional behavior, with a decreasing temperature differences between the two layers. This marks the start of the cooling of surface water due to increased mechanical and thermal convection.

In summary, the thermal stratification in the Baltic Sea shows a considerable variation among the different basins with a clear seasonal feature. During the winter period, the lower water layers are warmer than the upper layers. The ice starts to melt in late spring but still maintains a higher water temperature in the bottom layers. The temperature of the upper water layers starts to increase as the end of the summer approaches. By then, the upper water layers have a higher temperature and the stratification is reversed.

The common thermal stratification features in the Baltic Sea are obtained by analyzing the transient plots along all the cross sections:

1. The number of the stratified layers varies from two to five.
2. There are two distinct layers, one with lower surface temperature, i.e., winter stratification and a reversed summer-type stratification with higher surface temperatures. These two types prevail during winter–spring and summer–autumn, respectively. Typical transitional behavior may begin in late autumn, when the wind speed increases, but does not last more than a couple of weeks. These stratification features dominantly occur in shallower regions of the Baltic Sea.
3. The surface layer has a transient structure composed of two to three minor thermoclines with a mean thickness of about 10 m. It is often difficult to distinguish between these layers. Here, the thermocline layer is considered as a layer with temperature variations more than 0.4 °C, which gives negligible density difference (i.e., 0.01 kg/m³). The thermocline is located at a depth of 10–30 m.
4. The summer stratification has a dicothermal character in the northern basins of the Baltic Sea. This implies the existence of a colder layer sandwiched between two layers of higher temperatures. The layer is stable since the upper layer has a lower salinity than the deep underlying layer.

The foregoing features are shown in Figures 13 and 14 at two typical cross sections of S64 and S116, respectively. The former crosses most of the major basins in the Baltic Sea. This plot does not do justice to the complexity of the stratification in the Baltic Sea. The intention is to provide support to the results and the discussion. For thermal stratification, the layers are numbered in descending order from the surface (Table 2). The division was needed due to the complex nature of the multilayered thermal stratification. Layer 1 is defined as the surface or the top layer and the last layer refers to the bottom layer. It is not very useful to list the absolute values due to the significant geometric variations within and among the basins (size, volume, and depth).

Table 2. Characteristics of thermal stratification in the basin system of the Baltic Sea, 2000–2009.

Basins	Layers	Winter		Spring		Summer		Autumn	
		T °C	L _n %	T °C	L _n %	T °C	L _n %	T °C	L _n %
Bay of Bothnia	1	0.5	65	1.2	5	11	10	13.5	5
	2	0.5–1.5	23	1.2–0.8	5	11–3	30	13.5–3	35
	3	1.5	12	0.8	80	3–2	50	3–2	50
Sea of Bothnia	1	1.5	12	4.5	4.5	14–11.2	3	12	10
	2	1.5–3	33	4.5–1	13.5	11.2–3.2	25	12–2.5	20
	3	3	55	1.3	82	3.2–1.5	9	2.5–2	10
	4					1.5–3	40	2–3	47
	5					3	23	3	13
Gulf of Finland	1	0.2–0.25	42	7.5–1.5	42	16.2	21	13–12.8	21
	2	0.25–2.6	42	1.5	16	16.2–2.6	50	12.8–3.5	50
	3	2.6	16	1.5–4.2	42	2.6–4.2	29	3.5	29
Sea of Åland	1	0.5–4	25	4	10	14.2	10	10	10
	2	4–4.3	35	4–2.4	27	14.2–6.5	27	10–9	18
	3	4.3–4.8	40	2.4	27	6.5–3.9	63	9–5	72
	4			2.4–2.9	36				
Northern Gotland	1	4.2	43	6	8	16.2	5	13.5	10
	2	4.2–5.2	10	6–3.2	12	16.2–16.8	5	13.5–14.2	10
	3	5.2	47	3.2–2.8	11	16.8–16	10	14.2–3.5	20
	4			2.8–4.8	29	16–3	20	3.5–5	15
	5			5.5	40	3–4.8	16	5	35
	6					4.8	42		
Western Gotland	1	2	3	7–2.6	12	16–3.2	12	13.5	8
	2	2–5	20	2.6–5	18	3.2–5	11	3.5	4
	3	5–5.2	77	5–5.2	70	5–5.2	77	3.5–5	11
	4							5–5.2	77
Eastern Gotland	1	3.8	28	9–3	19	16.5	10	14	9
	2	3.8–6	33	3	13	16.5–3.7	10	14–3.7	9
	3	6–6.3	39	3–6	35	3.7–3	12	3.7–3	9
	4			6–6.3	33	3–6	26	3–6	28
	5					6–6.2	42	6–6.2	45
Bornholm Basin	1	4.5	55	12–4	33	17–16.5	28	15–14.8	18
	2	4.5–10	22	4	22	16.5–4.7	28	14.8–4.7	27
	3	10	23	9	33	7–6.2	16	4.7–7.8	22
	4			9–9.2	12	6.2–8	28	7.8–8.5	33
Arkona Basin	1	4	25	13.2–5.2	76	16.5	25	17–16.2	50
	2	4–4.5	25	5.2–4.8	23	16.5–8.5	25	16.2–8.8	25
	3	4.5–6	50			8.5–10.7	50	8.8–10.5	25

In the Bay of Bothnia, there is a significant seasonal variation regarding the number and thickness of the layers. The stratification in the Åland Sea is dominated by a three-layer structure, with the exception of a four-layer structure during the spring period. The stratified structure in the Gulf of Finland consists of three layers with significant variations in both thickness and temperature. The multilayered stratification structure for the Northern Gotland Basin is composed of top and bottom layers with constant temperatures. The Western Gotland Basin shows a sustained three-layered structure from the winter to summer period. The Eastern Gotland Basin stratification is similar to the northern basin except that the water temperatures are higher by 1 °C during the spring and autumn periods. The Bornholm Basin features are similar to the Eastern Gotland Basin. The Arkona Basin has a clear three-layer structure and during the winter and summer periods, the temperatures are constant in the 10-m thick upper layer, i.e., 4 °C and 16.5 °C, respectively. A short summary of each basin is reported in this paper. A detailed description of each basin’s stratification is given in Dargahi and Cvektovic [9]. The foregoing results are summarized in Table 2.

The seasonal variation in surface and bottom layer salinities is shown in Figures 15 and 16, respectively. Figures 17 and 18 show salinity contours for the years 2000 and 2006 as two typical years in the 10-year simulation period of 2000–2009. The general features are an outgoing surface flow with low salinity that is diluted by the fresh water from the rivers and a denser incoming bottom flow from the North Sea. The surface salinity varies from 1.6‰ to 9‰ and the bottom salinity in the range 3‰–16‰, moving southwards from the Bay of Bothnia to the Arkona Basin. The corresponding salinity gradients are 0.0042‰/m and 0.0054‰/m, respectively. The intruded high salinity water from the North Sea propagates like a plume as far as the Northern Gotland Basin, with a mean advection velocity of 6 cm/s. The feature is apparent from Figures 13, 14, 17 and 18, which show the dense water settling mainly in the deep regions of the Northern and Eastern Gotland Basins. The salinity

stratification has a multi-layer structure similar to the thermal stratification shown in Figures 13 and 14. The general features are two thick (i.e., >30 m) surface and bottom layers with a transition layer in-between. The stratification is complicated by its temporal and spatial variations both within and among the basins. A detailed discussion on salinity stratification is provided by Dargahi and Cvektovic [9] for all basins and so will not be repeated here. As an example, salinity stratification is briefly discussed for the Gulf of Finland and the Northern Gotland Basin.

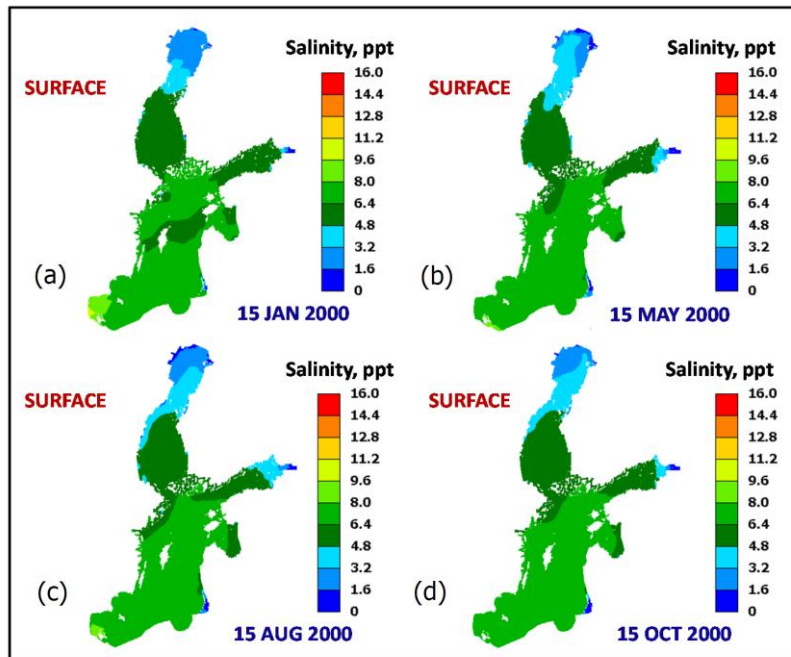


Figure 15. Seasonal plots of surface salinity in the Baltic Sea for the year 2000. (a) Winter; (b) Spring; (c) Summer; (d) Autumn.

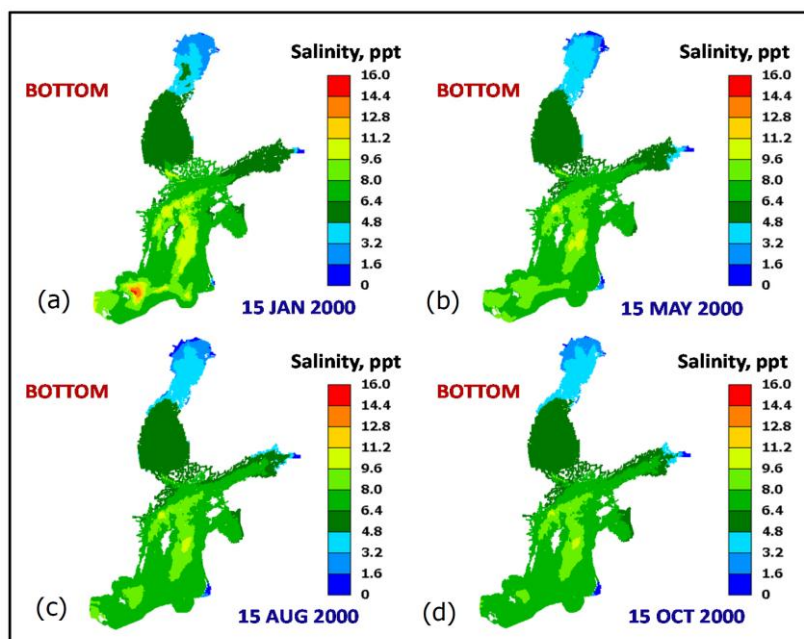


Figure 16. Seasonal plots of bottom salinity in the Baltic Sea for the year 2000. (a) Winter; (b) Spring; (c) Summer; (d) Autumn.

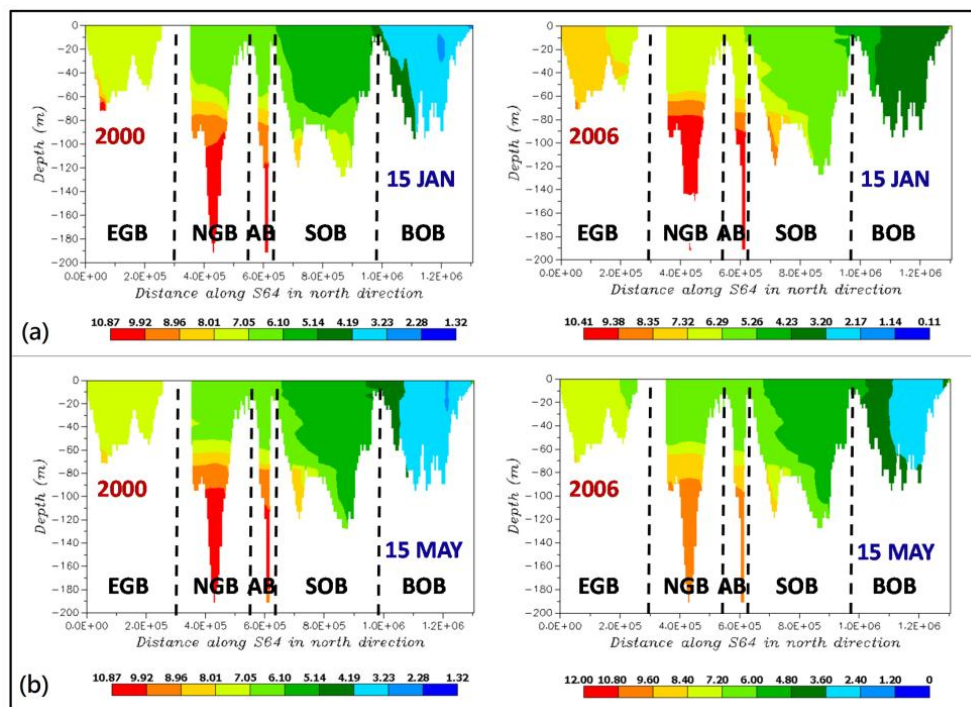


Figure 17. (a) Winter salinity stratification in the Baltic Sea at cross section S64 for the years 2000 and 2006; (b) Spring salinity stratification in the Baltic Sea at cross section S64 for the years 2000 and 2006.

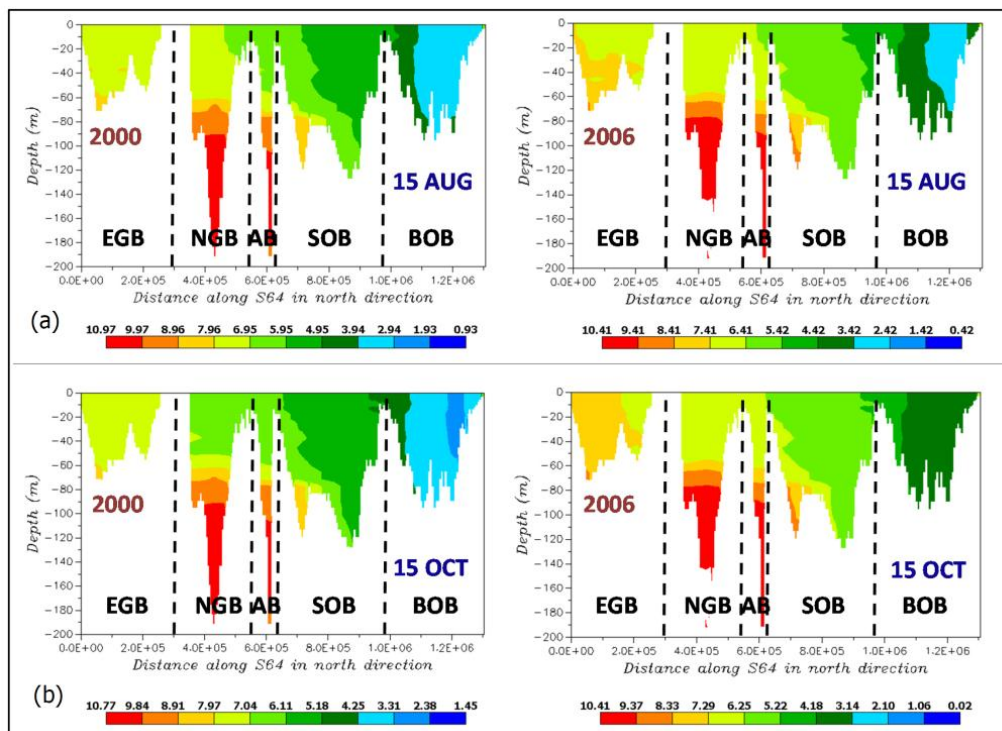


Figure 18. (a) Summer salinity stratification in the Baltic Sea at cross section S64 for the years 2000 and 2006; (b) Autumn salinity stratification in the Baltic Sea at cross section S64 for the years 2000 and 2006.

4. Discussion

The understanding of stratification in large water bodies is of significant environmental importance due to its direct coupling with water quality dynamics. Severe thermal stratification can

have a number of adverse effects, among which are reduced water quality and the spatial distribution of fish [41]. Any prolonged stratification can reduce oxygen solubility, which leads to oxygen depletion in deep water masses. The deeper water masses in the Baltic Sea are particularly vulnerable to eutrophication below the halocline or in regions affected by thermal stratification [42]. We know that eutrophication is the most serious and challenging environmental problem for the Baltic Sea [1]. Consequently, accurate knowledge of stratification dynamics is required for the management of eutrophication in the Baltic Sea.

The river Neva, the most voluminous river entering the Gulf of Finland (referred as Gulf in the foregoing discussion) from the eastern coastline (2500 m³/s), significantly affects the stratification in the Gulf. The zero-salinity water from the river creates a permanent plume that propagates westwards to a distance of 50–150 km. The plume salinity varies from 0% to 5% and extends to a depth of about 15 m. The maximum extension occurs during early spring periods. The seasonal cross section plots are shown in Figure 14 at S116 for the year 2000. The stratification in the Neva region appears to have a permanent multi-layer structure with few seasonal variations. The characteristic three-layer structure is found in the inner Gulf region. The stratification characteristics in the Northern Gotland Basin are similar to those in the inner Gulf region. It is interesting to note the significant salinity increase to 9.5% that is confined to the Northern Gotland Basin and the bottom layer.

The model prediction of three-layered salinity stratification in all basins of the Baltic Sea is in general agreement with previous studies [8]. Salinity stratification has a strong seasonal variability but is much weaker than the corresponding variability in temperature. The summary of model-predicted salinity data for the entire 10-year period into seasonal normalized layer thicknesses is shown in Table 3. The normalized values are more applicable than the absolute values given in the literature as the layer thicknesses could be estimated as a function of depth. The latter vary significantly within and among the basins. To examine the validity of the generalization, we compared the model and measured salinities at all stations and found good agreement between the data. An example is given in Table 4, which compares model results with measurements at station C3 (located in the Sea of Bothnia; see Figure 3) for the year 2000. Evidently, the predicted mean thicknesses are within the range of the measured data that supports our generalization.

Table 3. Characteristics of salinity stratification in the basin system of the Baltic Sea, 2000–2009.

Basins	Layers	Winter L_n %	Spring L_n %	Summer L_n %	Autumn L_n %	Salinity ‰
Bay of Bothnia	Upper	18	34	31	22	3
	Halocline	33	15	22	66	3.2
	Bottom	49	51	41	12	4
Sea of Bothnia	Upper	50	15	5	15	5
	Halocline	35	65	70	70	5.5
	Bottom	15	20	25	15	6.5
Sea of Åland	Upper	15	10	10	10	5.9
	Halocline	35	50	46	40	7.6
	Bottom	50	40	44	50	10
Gulf of Finland	Upper	25	32	25	30	4.7
	Halocline	30	38	50	40	6.5
	Bottom	45	40	25	30	8.3
Northern Gotland	Upper	35	38	20	25	5
	Halocline	30	32	55	45	42
	Bottom	35	30	25	30	28
Western Gotland	Upper	35	50	55	50	6.9
	Halocline	50	40	30	30	8.1
	Bottom	15	10	15	20	10
Eastern Gotland	Upper	30	20	25	20	6.8
	Halocline	35	50	50	55	9.3
	Bottom	35	30	25	25	11.5
Bornholm Basin	Upper	45	35	50	50	7.8
	Halocline	10	30	35	30	12.5
	Bottom	45	35	15	20	15.5
Arkona Basin	Upper	35	60	38	60	8
	Halocline	50	25	50	25	9
	Bottom	15	15	12	15	12

Table 4. Comparison of modeled and measured salinity stratification at station C3 (Sea of Bothnia), 2000.

Period	Upper Layer (m)		Halocline (m)		Bottom Layer (m)	
	Measured	Model	Measured	Model	Measured	Model
Winter	60–90	100	50–90	62	10–40	30
Spring	10–20	18	100–125	135	20–50	30
Summer	10–15	10	110–140	140	20–50	33
Autumn	15–30	22	100–130	127	20–45	22

The detailed investigation of thermal stratification for a 10-year period (i.e., 2000–2009) revealed some new features. The current study revealed a multilayered structure that contains several thermocline and dicothermal layers. The statistical analysis of all simulation results made it possible to derive the mean thermal stratification properties, expressed as mean temperatures and the normalized layer thicknesses (Table 2). The three-layered structure reported by Leppäranta and Myrberg [7] appears to be oversimplified.

The thermocline layer has a sharp temperature gradient that connects the upper and lower two layers. We have found the three-layer model to be valid only during the winter. In the northern basins, the vertical temperature gradients are significantly lower than for the southern basins (a factor 3). We attribute the difference to the formation of an ice cover during winter and spring in the northern basins (i.e., Northern Gotland Basin and above), which affects the surface heat transfer and its exchange with the overlying cold air. The ice layer acts as a thermal barrier preventing further heat losses due to the action of wind and convective transport. Consequently, the upper layer is rather thick and can occupy up to 65% of the depth in these basins. Following the winter, the three-layered structure is decomposed into several layers with increasing or decreasing temperature gradients. The process takes place in all the basins in the Baltic Sea. Here, we believe the primary driving force is the increased mixing processes between the basins during the ice-free periods. The high-momentum fresh water inflows from the rivers contribute to higher surface water temperatures, thus increasing the temperature gradients. On average, the thickest layer is the bottom layer ($\approx 50\%$) with a small temperature gradient, except in the Bornholm and Arkona basins. We believe the low gradients are due to low-intensity exchange processes in the northern basin of the deep water regions.

The Bornholm and Arkona basins are shallower and more influenced by the exchange of warmer and more saline waters with the North Sea. This is reflected by the increased temperature gradients in these basins (from ≈ 0.02 °C/m to ≈ 0.5 °C/m). Our simulations indicate a wide spectrum in the layering properties among the basins. However, a few generalizations appear to be possible based on the results listed in Table 2. The thermocline occupies about 25% of the water depth in each basin. The deep bottom layer is about 40% of the water depth with temperatures of about 3 °C and 5 °C in the northern and southern basins, respectively. Our mean results on the properties of thermal stratification agree well with the results reported by Leppäranta and Myrberg [7]. Here, the reported annual averaged halocline thickness is 10–20 m. For example, in the Bay of Bothnia we get an averaged normalized depth of 35% from Table 2. The mean depth is 40 m, which yields a thickness of 14 m—well within the range given by Leppäranta and Myrberg [7].

There is also some evidence of upwelling and downwelling along the coastlines across the Baltic Sea [3,6,39,43]. The existence of the dicothermal layer is an indication of upwelling. The two features occur as wind causes surface water to diverge (Ekman transport) or converge (downwelling). During both processes, water is either replenished from the deep region or forced downwards [44]. Consequently, the salinity variations, which are mainly controlled by the water balance, are further modified.

We will also examine the validity of having normalized layer thicknesses (Table 2) in each basin that only vary seasonally. We start by examining the measured vertical temperature profiles for two extreme locations of F3 (Bay of Bothnia) and BY5 (Bornholm Sea). Figure 19 shows the measured vertical temperature profiles at F3, and BY5 for the years 2000, 2008, and 2009. Note that the data were rather limited and thus the lines are only illustrative and do not necessarily show the correct trends.

The good agreement with the simulated summary results listed in Table 2 is apparent. For example, Table 2 predicts a thick top layer in the winter period (red line) at both stations that agrees well with the plots for F3, on 27 January 2000, and BY5, on 19 January 2000. We can also note that the profile shapes are preserved during the simulation period. However, the magnitudes of the temperatures show some significant variation. In conclusion, we believe the normalized layer thicknesses give reasonable estimates, with a standard deviation of $\pm 15\%$.

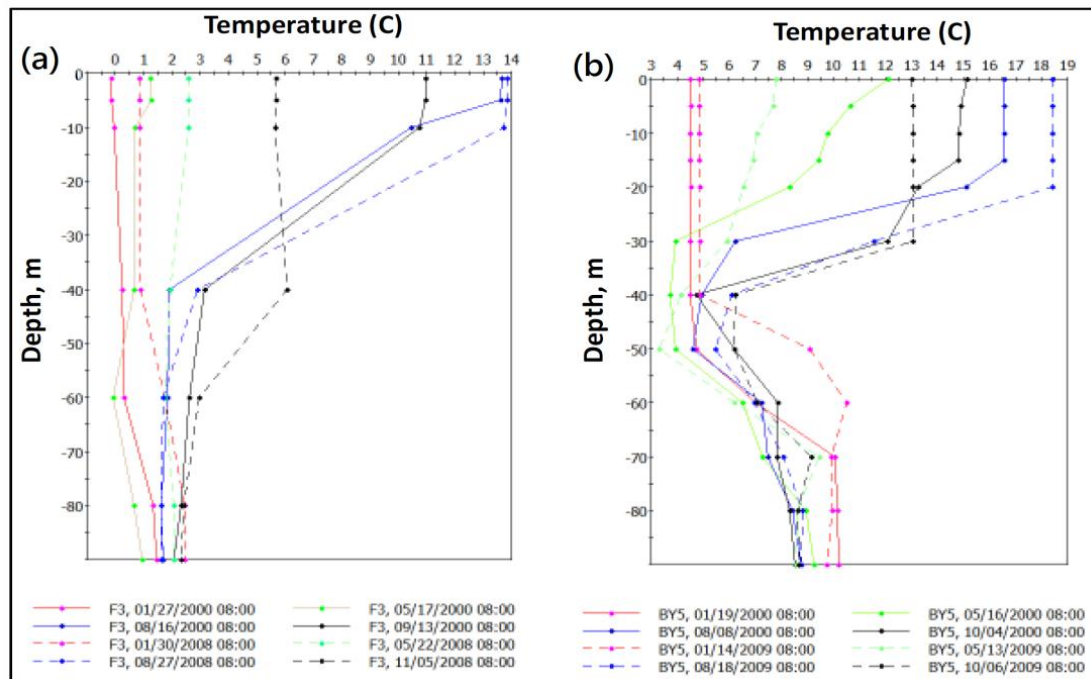


Figure 19. (a) Measured temperature profiles at F3 in 2000, 2008 and 2009; (b) Measured temperature profiles at BY5 in 2000, 2008 and 2009.

An interesting feature is the extreme inflow event of January 2003. According to Lehmann et al. [45], a massive salt intrusion of cold and oxygen-rich water from the North Sea took place at Darss Sill, which is a few kilometers west of the open sea boundary used in the model domain (see Figure 1). They consider the event as “the most important inflow from 1993”. Their results indicate significant changes in both salinity and temperature distributions in the deeper basins of the Baltic Sea. In the present study, we have investigated the reported event by comparing the surface and bottom salinities at all the stations (see Figure 3). We present the results in Figure 20, illustrating the salinity time series at stations BY1, BY5, and BY15 at the surface and bottom layers. The curves at BY1 are measured field data but the curves at BY5 and BY15 are model results. The model results are plotted at seven-day intervals for ease of comparison with the field data. Several important features are evident from this figure:

1. The event took place on 18 January 2003 with a salinity of 29%.
2. It took nearly a month for the peak salinity to reach station BY5, which dropped to 19%.
3. The peak salinity was reduced to 12.5% at station BY15 after almost five months.

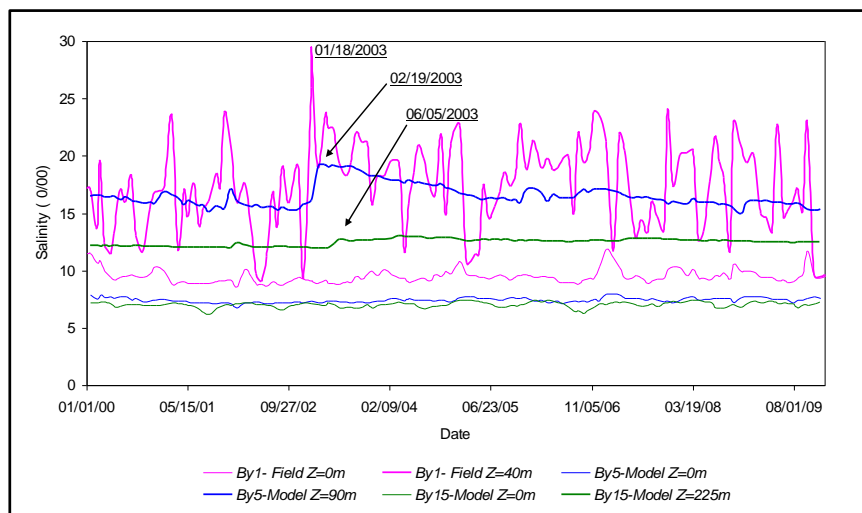


Figure 20. Time series of surface and bottom salinities at stations BY1, BY5, and BY15.

We computed the horizontal diffusive ($\theta_D \frac{\partial C^2}{\partial x^2}$) and advective transports ($U_m \frac{\partial C}{\partial x}$) using the foregoing information and the distances between the three stations (Table 5). A representative diffusion coefficient (θ_D) for the Baltic Sea is $10^3 \text{ m}^2/\text{s}$ [7]; the advective velocity is typically 0.1 m/s in the Arkona and Bornholm basins (present study). We can conclude that the diffusive transport is much faster than the advective transport. There is a significant reduction in the Eastern Gotland Basin in both modes of transport. It is interesting to note that the temporal variations in the bottom salinity appear to be random as opposed to the surface salinities. The surface salinities have lower amplitudes with no corresponding peaks as the bottom salinity. We believe the outgoing freshwater plays a significant role in lowering the salinity amplitude.

Table 5. Estimates of salinity transport in the southern basins.

Transport of Salt	BY1 (Arkona)-BY5 (Bornholm)	BY5-BY15(Eastern Gotland)
Diffusive (‰/day)	17×10^{-3}	5×10^{-3}
Advective (‰/day)	86×10^{-8}	1.12×10^{-8}

5. Conclusions

An integrated 3D modeling system was developed for the Baltic Sea using a public domain model called GEMSS[®]. The model was calibrated and verified using 10 years of data covering 2000–2009. We have incorporated boundary conditions and bathymetry with as high an accuracy as possible, to serve as an improvement over previous studies. The model was then used to investigate the vertical structure of the Baltic Sea to understand the stratification and exchange processes across various basins. This paper addressed in detail both the thermal and salinity stratifications, with a focus on the structural properties of the layers.

The hypothesis was that the layer properties could be expressed as dimensionless numbers valid for all seasons. In particular, the detection of cooler regions (dicothermal) within the layer structure has been an important finding. The detailed investigation of thermal stratification for a 10-year period (i.e., 2000–2009) revealed some new features. A multilayered structure that contains several thermocline and dicothermal layers prevails. Statistical analysis of the simulation results made it possible to derive the mean thermal stratification properties, expressed as mean temperatures and the normalized layer thicknesses.

The three-layered structure reported in the literature appears to be rather simplified. The current study found that the three-layer model is valid only during the winter.

The layering properties vary significantly among the basins whereby the layered structure could not be generalized. Nevertheless, a few generalizations appear to be possible. The thermocline occupies about 25% of the water depth in each basin. The deep bottom layer is about 40% of the water depth, with temperatures of about 3 °C and 5 °C in northern and southern basins, respectively.

Three-layered salinity stratification prevails in all basins of the Baltic Sea, in general agreement with previous studies. Salinity stratification has a strong seasonal variability but this is much weaker than the corresponding variability in temperature. We have succeeded in generalizing the seasonal normalized layer thicknesses for the entire 10-year period. The use of normalized values is advantageous compared to the absolute values given in the literature, enabling estimation of layer thickness as a function of depth.

This study provides detailed insight into thermal and salinity stratifications in the Baltic Sea during a recent decade and can be used as a basis for diverse environmental assessments (e.g., anoxia and reduced nutrient mixing between layers [1]). It extends previous studies on stratification in the Baltic Sea regarding both the extent and the nature of stratification.

Acknowledgments: This study was initiated and the first stage financed by the Central Baltic Interreg IV Programme as part of the project “Phosphorous from the seabed and water quality in archipelagos—modeling attempt (SEABED)”. The second stage of this study was funded by KTH Royal Institute of Technology, Division of Water Resources Engineering and Division of Hydraulic Engineering. The third and final stage of this study was funded by the project “The Baltic Sea Region System (BALSYS)”.

Author Contributions: The Baltic Sea hydrodynamic modeling study was done entirely by Bijan Dargahi. The original manuscript was prepared by Bijan Dargahi. The GEMSS model was developed by Venkat Kolluru. He also provided GEMSS model training for this study. The subsequent manuscript revisions and refinement of graphics were prepared by Venkat Kolluru. The project management and funding from three different sources were managed by Vladimir Cvetkovic.

Conflicts of Interest: The authors declare no conflict of interest.

References

- World Atlas. Available online: <http://www.worldatlas.com/aatlas/infopage/balticsea.htm> (accessed on 12 December 2016).
- Elmgren, R.; Larsson, U. *Himmerfjärden: Changes in a Nutrient-Enriched Coastal Ecosystem in the Baltic Sea*; Report 4565; Swedish Environment Protection Agency: Naturvårdsverket, Stockholm, Sweden, 1997.
- Meier, M. On the parameterization of mixing in three-dimensional Baltic Sea models. *J. Geophys. Res.* **2001**, *106*, 30997–31061. [[CrossRef](#)]
- Lehmann, A.; Hinrichsen, H.H. Water, heat and salt exchange between the deep basins of the Baltic Sea. *Boreal Environ. Res.* **2002**, *7*, 405–415.
- Omstedt, A.; Elken, J.; Lehmann, A.; Piechura, J. Knowledge of the Baltic Sea physics gained during the BALTEX and related programmes. *Progress Oceanogr.* **2004**, *63*, 1–28. [[CrossRef](#)]
- Feistel, R.; Nausch, G.; Wasmund, N. *State and Evolution of the Baltic Sea, 1952–2005: A Detailed 50-Year Survey of Meteorology and Climate, Physics, Chemistry, Biology, and Marine Environment*, 1st ed.; John Wiley & Sons, Inc.: Hoboken, NJ, USA, 2008.
- Leppäranta, M.; Myrberg, K. *Physical Oceanography of the Baltic Sea*, 1st ed.; Springer: Berlin, Germany, 2009.
- Harff, J.; Björck, S.; Hoth, P. *The Baltic Sea Basin*, 1st ed.; Central and Eastern European Development Studies; Springer: Berlin, Germany, 2011.
- Dargahi, B.; Cvetkovic, V. *Hydrodynamics and Transport Characterization of the Baltic Sea 2000–2009*, 1st ed.; TRITA-LWR REPORT 2014:03; KTH Royal Institute of Technology, School of Architecture and the Marine Environment: Stockholm, Sweden, 2014.
- Bock, K.H. Monthly salinity maps of the Baltic Sea for different depths. *Deutsche Hydrogr. Z.* **1971**, *12*, 1–147.
- Väli, G.; Meier, H.E.; Elken, J. *Simulated Variations of the Baltic Sea Halocline during 1961–2007*; Report Oceanography; Swedish Meteorological and Hydrological Institute (SMHI): Stockholm, Sweden, 2012; No. 44; pp. 1–37.
- Suominen, T.; Tolvanen, H.; Kalliola, R. Geographical persistence of surface-layer water properties in the Archipelago Sea, SW Finland. *Fennia* **2010**, *188*, 179–196.

13. Hordoir, R.; Meier, H.E.M. Effect of climate change on the thermal stratification of the Baltic Sea: A sensitivity experiment. *Clim. Dyn.* **2012**, *38*, 1703–1713. [[CrossRef](#)]
14. Fonselius, S. History of hydrographic research in Sweden. *Proc. Estonian Acad. Sci. Biol. Ecol.* **2001**, *50*, 110–129.
15. Peter, B. Dicothermal Layer Characteristics—A Case Study in the Antarctic Zone of Indian Ocean. *Proc. Indian Natl. Acad. Sci. USA* **1993**, *59*, 439–447.
16. SMHI. Swedish Meteorological and Hydrological Institute. Available online: <http://www.smhi.se/en> (accessed on 25 February 2012).
17. FMI. Finnish Meteorological Institute. Available online: <http://en.ilmatieteenlaitos.fi/> (accessed on 10 April 2012).
18. Leibniz Institute for Baltic Sea Research Warnemunde. Available online: <http://www.io-warnemuende.de/topography-of-the-baltic-sea.html> (accessed on 20 September 2012).
19. GEMSS®. Available online: <http://www.gemss.com> (accessed on 10 August 2011).
20. Edinger, J.E.; Buchak, E.M. Numerical hydrodynamics of estuaries in estuarine and wetland processes with emphasis on modeling. In *Estuarine and Wetland Processes with Emphasis on Modeling*; Hamilton, P., Macdonald, K.B., Eds.; Plenum Press: New York, NY, USA, 1980; pp. 115–146.
21. Edinger, J.E.; Buchak, E.M. Numerical waterbody dynamics and small computers. In Proceedings of the ASCE Hydraulic Division Specialty Conference on Hydraulics and Hydrology in the Small Computer Age, Lake Buena Vista, FL, USA, 13–16 August 1985; American Society of Civil Engineers: Reston, VA, USA, 1985; pp. 13–16.
22. Kolluru, V.S.; Buchak, E.M.; Edinger, J.E. Integrated Model to Simulate the Transport and Fate of Mine Tailings in Deep Waters. In Proceedings of the Tailings and Mine Waste '98 Conference, Fort Collins, CO, USA, 26–29 January 1998; pp. 599–610.
23. Kolluru, V.S.; Buchak, E.M.; Wu, J. Use of Membrane Boundaries to Simulate Fixed and Floating Structures in GLLVHT. In Proceedings of the 6th International Conference on Estuarine and Coastal Modeling, New Orleans, LA, USA, 3–5 November 1999; Spaulding, M.L., Butler, H.L., Eds.; pp. 485–500.
24. Kolluru, V.S.; Edinger, J.E.; Buchak, E.M.; Brinkmann, P. Hydrodynamic Modeling of Coastal LNG Cooling Water Discharge. *J. Energy Eng.* **2003**, *129*, 16–31. [[CrossRef](#)]
25. Kolluru, V.S.; Fichera, M. Development and Application of Combined 1-D and 3-D Modeling System for TMDL Studies. In Proceedings of the Eighth International Conference on Estuarine and Coastal Modeling, Monterey, CA, USA, 3–5 November 2003; American Society of Civil Engineers: Reston, VA, USA, 2003; pp. 108–127.
26. Kolluru, V.S.; Prakash, S. Evaluation of Urbanization and Impacts on Water Quality in Nottawasaga Bay Using an Integrated 3-D Modeling Framework. In Proceedings of the 7th International Congress on Environmental Modelling and Software, San Diego, CA, USA, 15–19 June 2014; Ames, D.P., Quinn, N.W.T., Rizzoli, A.E., Eds.; Available online: <http://www.iemss.org/society/index.php/iemss-2014-proceedings> (accessed on 25 January 2013).
27. Mellor, G.L.; Yamada, T. Development of a turbulence closure model for geophysical fluid problems. *Rev. Geophys. Space Phys.* **1982**, *20*, 851–875. [[CrossRef](#)]
28. Umlauf, L.; Burchard, H. A generic length-scale equation for geophysical turbulence models. *J. Mar. Res.* **2003**, *61*, 235–265. [[CrossRef](#)]
29. Warner, J.C.; Sherwood, C.R. Performance of four turbulence closure methods implemented using a generic length scale method. *Ocean Model.* **2005**, *8*, 81–113. [[CrossRef](#)]
30. Okubo, A. Oceanic diffusion diagrams. *Deep-Sea Res.* **1971**, *18*, 789–802. [[CrossRef](#)]
31. Smagorinsky, J. General circulation experiments with the primitive equations. *Mon. Weather Rev.* **1963**, *91*, 99–164. [[CrossRef](#)]
32. Prakash, S.; Kolluru, V.S. Implementation of higher order transport schemes with explicit and implicit formulations in a 3-D hydrodynamic and transport model. In Proceedings of the 7th International Conference on Hydrosience and Engineering, Philadelphia, PA, USA, 10–13 September 2006; Available online: <http://web.abo.fi/seabed> (accessed on 10 June 2013).
33. Dargahi, B.; Cvetkovic, V. Hydrodynamic and transport properties of Saltsjö Bay in the inner Stockholm Archipelago. *J. Coast. Res.* **2010**, *27*, 572–584. [[CrossRef](#)]

34. Dargahi, B.; Setegn, S. Combined 3D hydrodynamic and watershed modelling of Lake Tana, Ethiopia. *J. Hydrol.* **2011**, *398*, 44–64. [[CrossRef](#)]
35. Environmental Resources Management. *GEMSS Software Technical Documentation*; ERM: Malvern, PA, USA, 2006.
36. Madsen, O.S.; Grant, W.D. Quantitative description of sediment transport by waves. In Proceedings of the 15th International Conference on Coastal Engineering, ASCE, Honolulu, HI, USA, 11–17 July 1976; pp. 1093–1112.
37. Myrberg, K.; Andrejev, O. Modelling of the circulation, water exchange and water age properties of the Gulf of Bothnia. *Oceanologia* **2006**, *48*, 55–74.
38. Palmén, E. Untersuchungen über die Strömungen in den Finnland umgebenden Meeren. *Soc. Sci. Fennica Comment. Phys. Math.* **1930**, *12*, 1–94.
39. Harmel, R.D.; Smith, P.K.; Migliaccio, W.; Chaubey, I.; Douglas-Mankin, K.R.; Benham, B.; Shukla, S.; Muñoz-Carpena, R.; Robson, B.J. Evaluating, interpreting and communicating performance of hydrologic/water quality models considering intended use: A review and recommendations. *Environ. Model. Softw.* **2014**, *57*, 40–51. [[CrossRef](#)]
40. SMHI Oceanography. Available online: <http://www.smhi.se/klimatdata/oceanografi/havsis> (accessed on 7 March 2012).
41. Lackey, R.T. Response of physical and chemical parameters to eliminating thermal stratification in a reservoir. *Water Resour. Bull.* **1972**, *8*, 589–599. [[CrossRef](#)]
42. Baltic Marine Environment Protection Commission. *The Baltic Marine Environment 1999–2002*; Baltic Sea Environment Proceedings, No. 87; HELCOM: Helsinki, Finland, 2003.
43. Myrberg, K.; Andrejev, O. Main upwelling regions in the Baltic Sea a statistical analysis based on three-dimensional modelling. *Boreal Environ. Res.* **2003**, *8*, 97–112.
44. Lehmann, A.; Krauss, W.; Hinrichsen, H.H. Effects of remote and local atmospheric forcing on circulation and upwelling in the Baltic Sea. *Tellus* **2002**, *54*, 299–316. [[CrossRef](#)]
45. Lehmann, A.; Lorenz, P.; Jacob, D. Modelling the exceptional Baltic Sea inflow events in 2002–2003. *Geophys. Res. Lett.* **2004**, *31*, 1–4. [[CrossRef](#)]



© 2017 by the authors; licensee MDPI, Basel, Switzerland. This article is an open access article distributed under the terms and conditions of the Creative Commons Attribution (CC-BY) license (<http://creativecommons.org/licenses/by/4.0/>).